ARTICLE

Iridium(I) Complexes Bearing Hemilabile Coumarin-Functionalised N-Heterocyclic Carbene Ligands with Application as Alkyne Hydrosilylation Catalysts

Mert Olgun Karataş,[a,b,c] Bülent Alıcı,[b,c] Vincenzo Passarelli,[a] Ismail Özdemir,[b,c] Jesús J. Pérez-Torrente,*[a] and Ricardo Castarlenas,*[a]

A set of iridium(I) complexes of formula IrCl($\kappa C, \eta^2$-I^{R}Cou$^{R'}$)(cod) or IrCl($\kappa C, \eta^2$-BzI^{R}Cou$^{R'}$)(cod) (cod = 1,5-cyclooctadiene; Cou = coumarin; I = imidazolin-2-carbene; BzI = benzimidazolin-2-carbene) have beeen prepared from the corresponding azolium salt and [Ir(μ-OMe)(cod)]$_2$ in THF at room temperature. The crystalline structures of **4b** and **5b** show a distorted trigonal bipyramidal configuration in the solid state with a coordinated coumarin moiety. In contrast, an equilibrium between this pentacoordinated structure and the related square planar isomer is observed in solution as a consequence of the hemilability of the pyrone ring. Characterization of both species by NMR was achieved at the low and high temperature limits, respectively. In addition, the thermodynamic parameters of the equilibrium, ΔH_R and ΔS_R, were obtained by VT ^{1}H NMR spectroscopy and fall in the range 22-33 kJ·mol^{-1} and 72-113 J·mol^{-1}·K^{-1}, respectively. Carbonylation of IrCl($\kappa C, \eta^2$-BzI^{Tol}Cou$^{7,8\text{-}Me2}$)(cod) resulted in the formation of a bis-CO derivative showing no hemilabile behaviour. The newly synthesised complexes efficiently catalyze the hydrosilylation of alkynes at room temperature with a preference for the β-(Z) vinylsilane isomer.

Introduction

Strength of metal-ligand interactions is one of the key factors to control the coordination environment of organometallic species involved in catalysis. In this context, hemilabile ligands play a dual role, providing vacant sites in the initiation step by decoordination of a weakly-bonded arm, and stabilizing active species by recoordination of the nucleophilic moiety at the end of the catalytic cycle.[1] Functionalised N-heterocyclic carbenes (NHCs) with pendant donor groups are remarkable examples of such hemilabile ligands.[2] As far as iridium complexes are concerned, NHC ligands incorporating varied functionalities into the NHC architecture, such as alkenyl-,[3] aryl-,[4] N-,[5] O-,[6] S-,[7] or P-donor[8] groups, have been recently described. Moreover, a range of catalytic transformations have taken advantage of the hemilabile effect including hydrogenation,[3a,b,5a,d,g,8b] isomerization of epoxides,[3d] C-H activation,[4a] hydroamination,[4b,5e,f,8a] reduction of nitroarenes,[5b] [3+2] cycloadditions,[5c] hydrogen borrowing tranformations,[5h,i] alcohol dehydrogenation,[6c] and, particularly, alkyne hydrosilylation.[3c,5f,6b] The latter reaction has become one of the most efficient methods for the preparation of vinylsilanes in terms of availability of reagents and full compliance with the atom economy principle.[9] However, the hydrosilylation of terminal alkynes can afford three vinylsilane isomers, namely, α-(Markovnikov), β-(E) and β-(Z) (both anti-Markovnikov). Additionally, dehydrogenative silylation, oligomerization and polymerization make the control of the regio- and stereoselectivity even more difficult. Therefore, although efficient transition metal-based catalysts have been

developed,[10] further research work is necessary in order to face these challenges.

In a previous study, we reported on the ability of coumarin-functionalized N-heterocyclic carbene ligands to stabilize penta-coordinated RhCl(NHC)$_2$ species through the coordination of the coumarin moiety that behaves similarly to an allyl group.[11] Although coumarin derivatives stand out due to their biological[12] and fluorescent[13] properties, the distinctive coordination of the α,β-unsaturated bond of the pyrone ring may render coumarin-functionalised NHCs as a smart structural motifs in coordination chemistry. In this connection, we have reported a zwitterionic Rh(III) complex with carboxylate-functionalized bis-NHC ligands as excellent alkyne hydrosilylation catalyst presenting high selectivity to β-(Z) vinylsilane.[14] DFT calculations suggested that the carboxylate fragment acts as a silane carrier which is essential for the excellent selectivity achieved. These promising results encouraged us to investigate if the keto group of the coumarin scaffold could play a similar role (Chart 1). Thus, herein we report on the synthesis of a series of iridium(I) complexes featuring coumarin-functionalised NHC ligands that exhibit a dynamic behaviour derived from the hemilability of the ligand. In addition, their performance as alkyne hydrosilylation catalysts has been investigated.
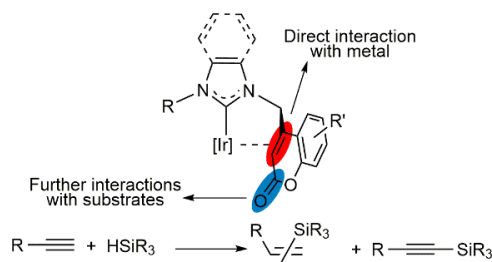
Chart 1. Potential interactions of NHC-coumarin-functionalised Iridium catalyst for alkyne hydrosilylation.

a. Departamento de Química Inorgánica-Instituto de Síntesis Química y Catálisis Homogénea (ISQCH), Universidad de Zaragoza-CSIC
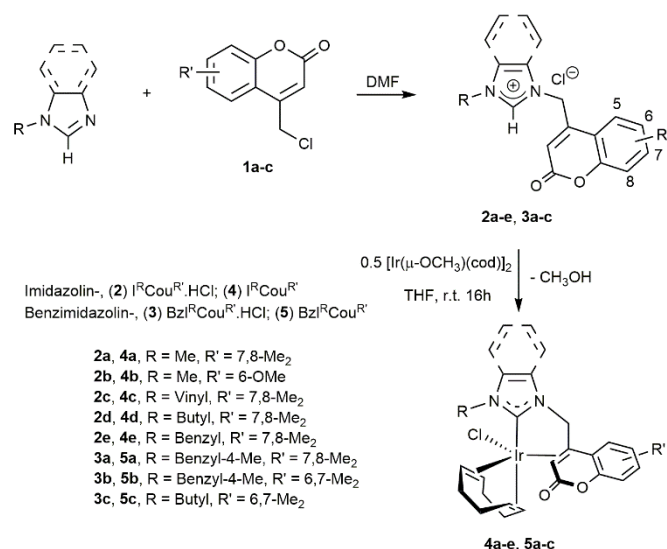C/Pedro Cerbuna 12, CP. 50009, Zaragoza (Spain)

b. Department of Chemistry, Faculty of Sciences, Inönü University, 44280, Malatya (Turkey)

c. Catalysis Reseach and Application Center, İnönü University, 44280 Malatya (Turkey)

Results and Discussion

### Synthesis and characterization of Ir(I)-NHC complexes

Coumarin-functionalised imidazolium (**2a-e**) and benzimidazolium (**3a-c**) chloride salts were synthesised by reaction of (4-chloromethylene)coumarin derivatives (**1**)[15] with the corresponding azole compound according to the previously reported method (Scheme 1).[11] Reaction of the azolium salts with [Ir(μ-OMe)(cod)]$_2$ (cod = 1,5-cyclooctadiene) in THF at room temperature for 16 hours gave the target complexes IrCl($\kappa C,\eta^2$-I^{R}Cou$^{R'}$)(cod) (**4a-e**) and IrCl($\kappa C,\eta^2$-BzI^{R}Cou$^{R'}$)(cod) (**5a-c**) which were isolated as orange solids in 49-72% yields.

Imidazolin-, (**2**) I^{R}Cou$^{R'}$.HCl; (**4**) I^{R}Cou$^{R'}$
Benzimidazolin-, (**3**) BzI^{R}Cou$^{R'}$.HCl; (**5**) BzI^{R}Cou$^{R'}$

2a, **4a**, R = Me, R' = 7,8-Me$_2$
2b, **4b**, R = Me, R' = 6-OMe
2c, **4c**, R = Vinyl, R' = 7,8-Me$_2$
2d, **4d**, R = Butyl, R' = 7,8-Me$_2$
2e, **4e**, R = Benzyl, R' = 7,8-Me$_2$
3a, **5a**, R = Benzyl-4-Me, R' = 7,8-Me$_2$
3b, **5b**, R = Benzyl-4-Me, R' = 6,7-Me$_2$
3c, **5c**, R = Butyl, R' = 6,7-Me$_2$

Scheme 1. Synthesis of coumarin-functionalised-NHC-Ir complexes.

The solid-state structures of **4b** and **5b** were determined by X-ray diffraction analysis on single crystals obtained by slow diffusion of *n*-hexane into concentrated CDCl$_3$ solutions (Figure 1). Both complexes show a pentacoordinate environment at the metal centre resulting in a distorted trigonal bipyramidal geometry (τ 0.66, **4b**; 0.65, **5b**).[16] The carbene carbon atom C1 and one cod olefinic bond (**4b**, C21-C22; **5b**, C32-C33) occupy the apical positions [C1-Ir1-ct2 173.10(12)°, **4b**; 175.08(13)°, **5b**], whereas the remaining cod olefinic bond (**4b**, C25-C26; 5b, C36-C37), the chlorido ligand Cl1 and the olefinic bond of the coumarin moiety (**4b**, C8-C9; **5b**, C11-C12) lie at the equatorial sites. Reasonably, as a consequence of the strong *trans* influence of the NHC moiety as well as of the higher steric hindrance at the apical positions when compared with the equatorial ones, the metal-centroid distance Ir1-ct2 [2.1796(2) Å, **4b**; 2.1744(2) Å, **5b**] is longer than Ir1-ct3 [2.0055(2) Å, **4b**; 2.0322(2) Å, **5b**]. Accordingly, the cod olefinic bond at the apical position [4b, C21-C22 1.373(6) Å; 5b, C32-C33 1.378(7) Å] is shorter than the cod olefinic bond at the equatorial position [**4b**, C25-C26 1.442(6) Å; **5b**, C36-C37 1.432(7) Å]. As far as the coumarin moiety is concerned, as a result of the coordination of the olefinic bond, the bond lengths C8-C9 [**4b**, 1.441(6) Å] and C11-C12 [**5b**, 1.439(6) Å] are approx. 0.09 Å longer than that observed in related rhodium-NHC complexes of formula RhCl(cod)(BzI$^{Bz-4-Me}$Cou$^{7,8-Me2}$) and RhCl(cod)(IBzCou$^{7,8-Me2}$)$_2$[11] featuring a non-coordinated coumarin wingtip. Remarkably, the metal complexes **4b** and **5b** are chiral, and according to the skew line system[17] the molecular structures shown in Figure 1 exhibits a $\varDelta$ configuration. Nonetheless, it is worth a mention that the space group of both **4b** (*P*21/*c*) and **5b** (*P*21/*n*) is centrosymmetric. As a result, the unit cell

contains the $\varLambda$ enantiomer as well, with an overall $\varDelta$:$\varLambda$ ratio of 1:1. Further, it should also be noted that when it comes to the coordinated coumarin moiety, the olefinic bond C8-C9 (**4b**) and C11-C12 (**5b**) can coordinate the metal centre via either the 3*si*,4*re* or the 3*re*,4*si* enantioface. Notably, the crystal structure of both **4b** and **5b** shows that the 3*si*,4*re* enantioface coordinates diastereoselectively to the metal centre in the $\varDelta$ enantiomer whereas the 3*re*,4*si* enantioface coordinates diastereoselectively to the metal centre in the $\varLambda$ isomer. This diasteroselectivity was previously observed in related rhodium compounds of formula RhCl(BzI^{Me}Cou$^{7,8-Me2}$)$_2$ and RhCl(I^{Me}Cou$^{7,8-Me2}$)$_2$ arguing that in that case it is the consequence of the relative stability of the possible diasteromers.[11] Finally, the reduced bite angle of both the I^{Me}Cou^{6-OMe} [**4b**, C1-Ir1-ct1 80.09(14)°] and BzI^{MeBz}Cou$^{7,8-Me2}$ [**5b**, C1-Ir1-ct1 80.53(14)°] brings about a significant deviation of the arrangement of the NHC moiety with respect to the Ir-C1 bond resulting in yaw angles[18] of 10.1° (**4b**) and 9.5° (**5b**), similar to those observed in the above mentioned rhodium compounds RhCl(BzI^{Me}Cou$^{7,8-Me2}$)$_2$ and RhCl(I^{Me}Cou$^{7,8-Me2}$)$_2$.[11]
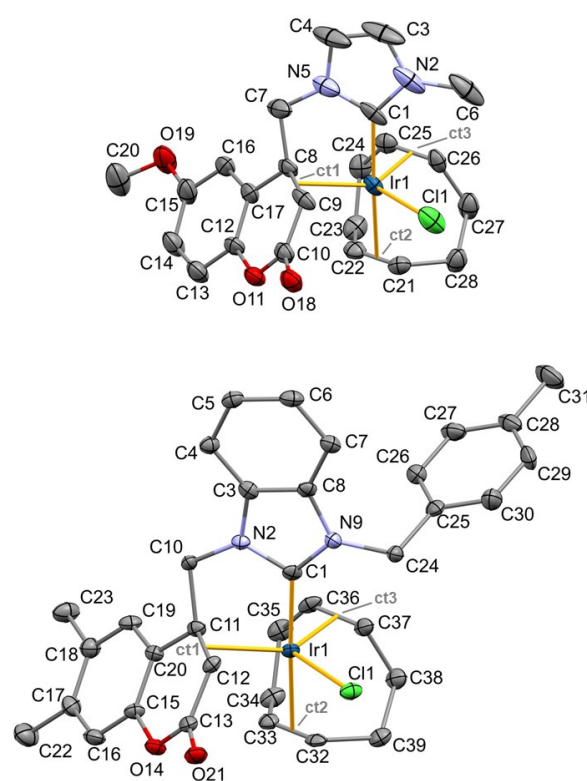
Figure 1. ORTEP view of the crystal structure of **4b** (*top, 2·CH$_3$Cl*) and **5b** (*bottom, 1.7·CH$_3$Cl*) with ellipsoids at 50% probability. Hydrogen atoms and lattice chloroform molecules are omitted for clarity. Selected bond lengths (Å) and angles (°) are: **4b**, C1-Ir1 2.015(5), Cl1-Ir1 2.4917(12), Ir1-ct1 2.0548(2), Ir(1)-ct2 2.1796(2), Ir(1)-ct3 2.0055(2), C8-C9 1.441(6), C21-C22 1.373(6), C25-C26 1.442(6), C1-Ir1-Cl1 88.78(15), C1-Ir1-ct1 80.09(14), C1-Ir1-ct2 173.10(12), ct1-Ir1-Cl1 108.10(3), ct1-Ir1-ct3 134.522(10), ct3-Ir1-Cl1 115.74(3); ct1, centroid of C8 and C9; ct2, centroid of C21 and C22; ct3, centroid of C25 and C26; **5b**, C1-Ir1 2.010(5), Cl1-Ir1 2.4999(12), Ir1-ct1 2.0610(2), Ir1-ct2 2.1744(2), Ir1-ct3 2.0322(2), C11-C12 1.439(6), C32-C33 1.378(7), C36-C37 1.432(7), C1-Ir1-Cl1 87.51(13), C1-Ir1-ct2 175.08(13), C1-Ir1-ct1 80.53(14), ct1-Ir1-ct2 102.781(9), ct1-Ir1-ct3 135.518(9), ct3-Ir1-Cl1 115.34(3), ct1-Ir1-Cl1 107.81(3); ct1, centroid of C11 and C12; ct2, centroid of C32 and C33; ct3, centroid of C36 and C37.

The NMR spectra of **4-5** agree with the structure observed in solid state. However, the ^{1}H NMR spectra at room temperature showed broad resonances, therefore low temperature measurements (213 K) were necessary for obtaining a sharp definition of the signals. Accordingly, the ^{1}H-^{1}H COSY, ^{13}C{^{1}H}-APT and ^{1}H-^{13}C HSQC/HMBC NMR spectra of all complexes were measured at 213 K. In the ^{1}H NMR spectra, the olefinic cod hydrogens of **4** and **5** were observed around 3.5 ppm, whereas the protons of the methylene linker of imidazolin-based complexes **4** appear around 4.8 and 3.7 ppm with geminal coupling constants of about 13.2 Hz. The corresponding methylene hydrogens of benzimidazolin-based complexes **5** appear slightly deshielded (≈ 4.9 and 4.0 ppm), displaying lower coupling constants (12.8 Hz). The [13]C{[1]H}-APT spectra also showed the set of signals expected for the proposed structure of the complexes. Thus, carbene carbon atoms of **4** appear around δ 156 ppm while that of the benzimidazolin derivatives **5** were found to be deshielded to about 168 ppm. In addition, carbonyl carbon atom of the coumarin moiety resonates around δ 168 ppm for both imidazolin and benzimidazolin complexes. Moreover, the two olefinic carbons of the pyrone ring were observed in the range of δ 53-38 ppm, in agreement with its coordination to the iridium centre. The remaining signals ascribed to cod and NHC ligands were also found at chemical shifts in accordance with the proposed structures.

In addition, variable-temperature ^{1}H NMR spectra were measured for selected complexes (**4a**, **4e**, and **5b**). Figure 2 displays the stacked ^{1}H NMR spectra for **5b** at different temperatures. An equilibrium between the pentacoordinated structure with metal-bonded coumarin (**5b**) and the square planar configuration displaying a monodentate NHC (**5b'**) can be inferred from the spectra, as a consequence of a hemilabile behaviour. On raising the temperature from 213 K the signals corresponding to the coumarin wingtip and cod broaden, reach the coalescence around 263-283 K, and become sharp again at 323 K. The more meaningful resonance is that of the =CH of the pyrone ring (red star in Figure 2) which was observed at δ 3.62 ppm at 213 K, while it shifted to 5.61 ppm at 343 K. The signals corresponding to the protons of the methylene linker between coumarin and imidazolin also shift from 4.02 and 5.05 ppm at 213 K to 6.67 and 5.66 ppm, with a concomitant increment of the geminal coupling constant from 12.8 to 17.5 Hz. The analysis of the dependence of the chemical shift of the =CH of the pyrone ring with the temperature allows for the determination of thermodynamic parameters of the equilibrium: ΔH_R = 29.4 ± 1 kJ·mol^{−1} and ΔS_R = 103.5 ± 4 J·mol^{−1}·K^{−1} (see Supporting Information). The high positive value of ΔS_R are in accordance with a more ordered structure for the isomer observed at low temperature. It is interesting to note that the equilibrium is totally shifted to pentacoordinated complex **5b** at 213 K whereas a molar ratio **5b':5b** of around 9:1 was calculated at 343K (see Supporting Information). The signals of NHC-carbon atoms in the [13]C{[1]H}-APT spectra follow the same trend (Figure 3). Thus, the =CH carbon of the pyrone ring shifts from the typical value of a coordinated ligand (δ 40.3 ppm) in **5b**, to a figure more characteristic of a free olefin in **5b'** (δ 95.2 ppm). Moreover, the carbene carbon atom is more deshielded at high temperature (167.6 ppm, 213 K *vs* 187.0 ppm, 323 K) in agreement with an increment of electron density on iridium center in the square planar conformation of **5b'**.[20] Similar thermodynamic parameters were calculated for the imidazolin-based complexes **4a** (ΔH_R = 22.6 ± 3 kJ·mol^{-1}, ΔS_R = 72.3 ± 13 J·mol^{-1}·K^{−1}) and **4e** (ΔH_R = 33.5 ± 8 kJ·mol^{-1}, ΔS_R = 117.6 ± 26 J·mol^{-1}) (see Supporting Information).
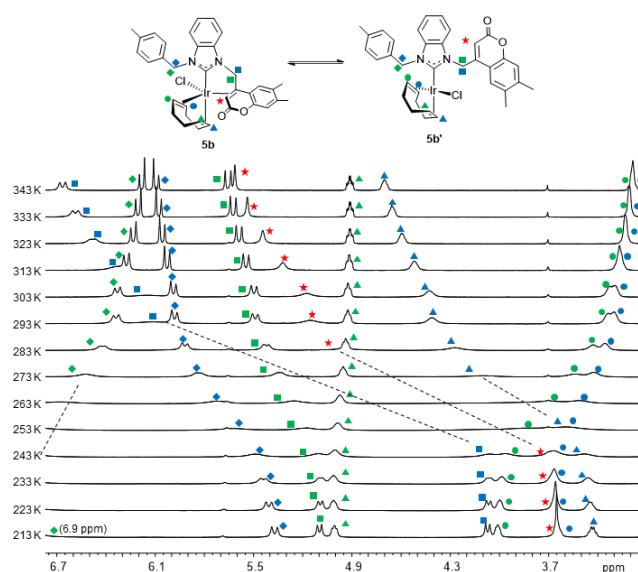
Figure 2. Selected region of the variable-temperature ^{1}H NMR spectra of the equilibrium mixture **5b ⇌ 5b'** in CDCl₃.
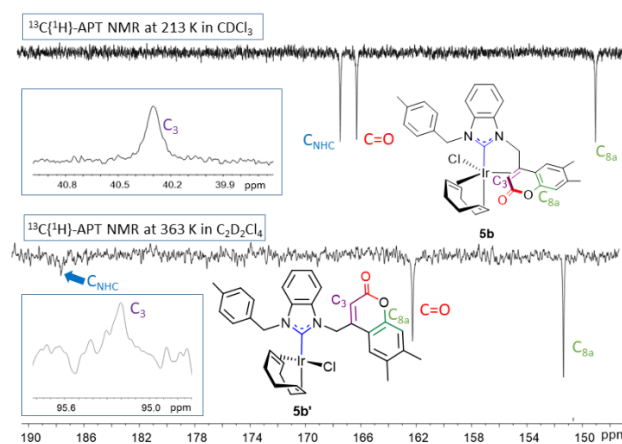
Figure 3. Selected regions of the [13]C{[1]H}-APT spectra of **5b** and **5b'**.

The bis-carbonyl complex IrCl(BzI[Tol]Cou[7,8-Me2])(CO)₂ (**6**) was synthesised by bubbling carbon monoxide through a solution of **5a** in THF and isolated in 54 % yield (Scheme 2). In contrast to **4-5**, the coordination of coumarin moiety to iridium was not observed even at 213 K, likely due to a higher π-acceptor capacity of CO ligands related to cod. Thus, the olefinic hydrogen of the pyrone ring of **6** resonates at δ 5.53 ppm in the ^{1}H NMR spectrum, deshielded about 2 ppm with regard to the related signals of diene counterparts **4-5**. The resonances ascribed to the protons of the methylene linker were observed as two doublets at 6.49 and 5.81 ppm with a coupling constant of 18.3 Hz. The [13]C{[1]H}-APT spectrum displays a singlet at δ 183.9 ppm corresponding to the carbene carbon atom, which is down-field shifted about 15 ppm compared to the cod complexes **4** and **5**. The carbonyl ligands were observed at δ 180.8 (located *trans* to NHC) and 167.3 ppm (*cis* to NHC). The olefinic carbons of the pyrone ring resonates at δ 149.2 and 110.9 ppm, thus discarding a η²-coordination to iridium center. In the IR spectrum of **6**, the wavenumbers of the symmetric and asymmetric CO stretching modes are 2059 cm^{-1} and 1981 cm^{-1}, respectively, which are in good agreement with the reported values for Ir-NHC complexes. As a result, it can be argued that imidazolin-, imidazolidin-, and

benzimidazolin-based NHCs have similar electron-donating capacity.[19]
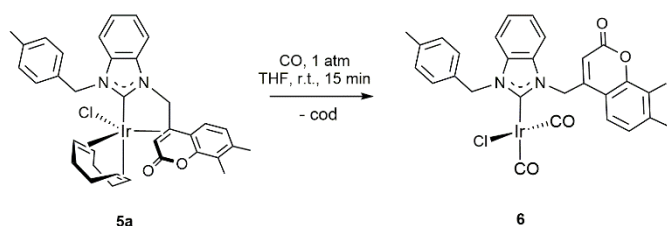
Scheme 2. Synthesis of the bis-carbonyl complex **6**.

Catalytic studies

The synthesized iridium(I) complexes bearing coumarin-functionalized NHC ligands (**4**-**6**) were screened as catalysts in the hydrosilylation of terminal alkynes using phenylacetylene (PA) and dimethylphenylsilane (HSiMe$_2$Ph) as representative substrates. The catalytic reactions were carried out under argon atmosphere in CDCl$_3$ at room temperature with a 2 mol% catalyst loading and a slight excess of hydrosilane. Additionally, for the sake of comparison, the catalytic activity of tetra- and pentacoordinated rhodium complexes related to **2d**, RhCl(NHC)(cod) (**7**) and RhCl(NHC)$_2$ (**8**),[11] was investigated for comparative purposes (Scheme 3). The results obtained from these preliminary experiments are outlined in Table 1.
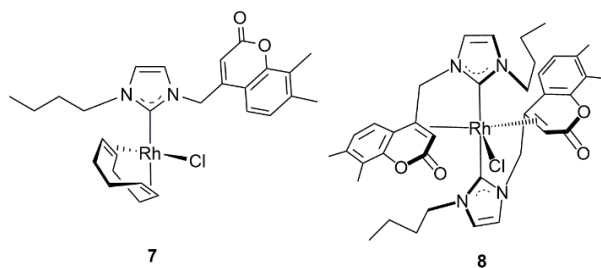
Scheme 3. Selected Rh(I)-NHC complexes tested as catalysts in hydrosilylation of terminal alkynes.

According to the results, the imidazolin-based complexes [IrCl(NHC)(cod)] (**4a-e**) efficiently catalysed the hydrosilylation of PA at room temperature reaching PA conversions higher than 95% in 4 h with 75-85% selectivity to the *β*-(*Z*)-vinylsilane product and variable amounts of the *β*-(*E*)-vinylsilane (10-15%) and α-vinylsilane isomers (2-4%) (entries 1-5). In addition, the formation of styrene, the dehydrogenative silylation by-product, has been observed to some extent. The benzimidazolin-based complexes [IrCl(NHC)(cod)] (**5a-c**) were found to be less active (**5b** and **5c**) or less selective to the *β*-(*Z*)-vinylsilane (**5a**) (entries 6-8). Additionally, it should be noted that the conversion of the *β*-(*Z*) isomer into the thermodynamically more stable *β*-(*E*)-vinylsilane isomer was not observed. In fact, all the imidazolin-based catalysts allow full PA conversion at longer reaction times (8-24 h) while maintaining the selectivity. In sharp contrast, the hydrosilylation of PA by the benzimidazolin-based carbonyl complex [IrCl(NHC)(cod)] (**6**) is unselective affording only a 45% conversion in 24 h (entry 9). Finally, the rhodium(I)-NHC complexes **7** and **8** did not show catalytic activity at room temperature. However, the hydrosilylation proceeded efficiently at 333 K attaining 96 and 86% conversions, respectively, in 4 h although with poor selectivity (entries 10-13).

Table 1. Hydrosilylation of PA with HSiMe$_2$Ph catalysed by Ir- and Rh-NHC complexes.[a]

Entry	Catalyst	Time (h)	Conversion[b] (%)	Selectivity (%)[b] β-(Z) / β-(E) / α / styrene[a]
1	**4a**	1	76	82 / 11 / 2 / 5
		4	>99	84 / 11 / 2 / 3
2	**4b**	1	61	79 / 14 / 2 / 5
		4	95	75 / 15 / 4 / 6
		24	>99	78 / 13 / 3 / 6
3	**4c**	1	58	84 / 9 / 2 / 5
		4	95	86 / 9 / 2 / 3
		24	98	87 / 8 / 2 / 3
4	**4d**	1	54	88/ 9 / 1 / 2
		4	97	75 / 16 / 3 / 6
		8	>99	75 / 15 / 3 / 7
5	**4e**	4	96	75 / 13 / 4 / 8
		24	>99	78 / 11 / 4 / 7
6	**5a**	4	93	66 / 18 / 4 /12
		8	97	57 / 27 / 5 /11
7	**5b**	4	58	79 / 12 / 4 / 5
		24	91	77 / 12 / 4 / 7
8	**5c**	4	69	82 / 14 / 1 / 3
		24	97	82 / 11 / 3 / 4
9	**6**	4	20	0 / 65 / 12 / 23
		24	45	14 / 51 / 10 /25
10	**7**	4	0	-
11	**7**[c]	4	96	36 / 26 / 25 /13
12	**8**	4	0	-
13	**8**[c]	4	86	42 / 46 / 3 / 9

[a] Experiments were carried out in CDCl$_3$ (0.5 mL) at room temperature using a HSiMe$_2$Ph/PA/catalyst ratio of 110/100/2, [catalyst]$_o$ = 8 mM. [b] Conversion and selectivities were determined by ^{1}H NMR. [c] Reaction was carried out at 333 K.

Compound **4a** has revealed as the most efficient catalyst precursor for the hydrosilylation of PA along this Ir-NHC series and, consequently, its performance in the hydrosilylation of selected aliphatic and aromatic terminal alkynes with different silanes has been studied (Table 2). The hydrosilylation of hex-1-yne with HSiMe$_2$Ph was complete in 4 h to afford a mixture of vinylsilanes in which the *β*-(*E*) and *β*-(*Z*) isomers predominate (entry 1). However, good selectivity for the *β*-(*Z*)-vinylsilane isomer (75-80%) was observed in the hydrosilylation of ring-substituted phenylacetylene derivatives having electronically dissimilar substituents at para position with HSiMe$_2$Ph (entries 2 and 3). Full conversion was achieved in the hydrosilylation of electron-rich alkynes such as 4-(methoxy)phenylacetylene in 4 h. Nevertheless, the hydrosilylation of electron-poor alkynes, such as 4-(trifluoromethyl)phenylacetylene, was slower reaching a 71% conversion in 4 h and quantitative conversion in 24 h with the same selectivity. In contrast, the functionalized 2-(ethynyl)pyridine derivative was unreactive under these conditions, likely due to the catalyst deactivation by coordination of the pyridine moiety (entry 4). Finally, the hydrosilylation of PA with HSiMePh$_2$ and HSiEt$_3$ was also studied (entries 5 and 6). Full PA conversion was attained using HSiMePh$_2$ in 24 h, albeit with moderate selectivity to the *β*-(*Z*)-vinylsilane isomer (entry 5). Although the hydrosilylation of PA with HSiEt$_3$ is slower, 81% PA conversion in 24 h, the *β*-(Z)-vinylsilane was obtained with 84% selectivity.

Table 2. Hydrosilylation of terminal alkynes catalysed by **4a**.

Entry	Alkyne	Silane	Time (h)	Conversion[a] (%)	Selectivity (%) β-(Z)/β-(E)/α/styrene[a]
1		HSiMe$_2$Ph	4	>99	37 / 40 / 6 / 17
2		HSiMe$_2$Ph	4	>99	82 / 14 / - / 4
3		HSiMe$_2$Ph	4	71	76 / 17 / 3 / 4
			24	>99	76 / 16 / 4 / 4
4		HSiMe$_2$Ph	24	-	-
5		HSiMePh$_2$	24	>99	58 / 35 / - / 17
6		HSiEt$_3$	24	81	84 / 10 / - / 6

[a] Experiments were carried out in CDCl$_3$ (0.5 mL) at room temperature using a HSiR$_3$/alkyne/catalyst ratio of 110/100/2, [**4a**]$_o$ = 8 mM. [b] Conversion and selectivities were determined by ^{1}H NMR.

Relevant to this discussion, recently, there has been an increasing interest in the development of alkyne hydrosilylation rhodium,[10c,21] and iridium[3c,5f,22] catalysts based on functionalized N-heterocyclic carbene ligands with hemilabile properties. Despite their moderate selectivity, the catalytic activity exhibited by the imidazolin-based Ir-NHC complexes is remarkable. In contrast to most of the Rh-NHC catalyst precursors, which show excellent catalytic activity at 50-60 ºC, compound **4a-4e** are active at room temperature at relatively low catalysts loading reaching around 60 % PA conversion in only 1 h (Table 1). The activity is comparable to that exhibited by IrCl(NHC)(cod) complexes featuring bis-allyl functionalized NHC ligands[3c] which highlight the positive influence of weak coordinating hemilabile groups on the catalytic activity.

Hydrosilylation of terminal alkynes by iridium catalysts usually affords the thermodynamically unfavorable β-(Z) vinylsilanes as the major products.[23] A notable exception is the catalytic system reported by Ding *et al*. which is selective to the Markovnikov α−vinylsilane reaction products.[24] The catalytic performance of our coumarin-functionalized Ir-NHC catalysts compares well with the moderate stereoselectivities observed for Ir(I) catalysts and fall behind when compared with the excellent selectivities achieved by Ir(III) catalysts.[25] As far as the operating mechanism is concerned, the selectivity attained by catalyst precursors **4** points to a modified Chalk-Harrod mechanism which accounts for the competitive dehydrogenative-silylation process occasionally observed with some rhodium and iridium catalysts.[26] However, reactivity studies have shown that **4a** does not react either with phenylacetylene or HSiMe$_2$Ph even a 60 ºC. Therefore, although we do not have experimental evidence, an ionic outer-sphere mechanism could be operating in which the pyrone functionality of the coumarin moiety might promote the heterolytic activation of the hydrosilane mediated by the iridium center, thus acting as a carrier of the silane moiety to the alkyne.[14, 27]

Conclusions

A series of iridium(I) complexes containing a coumarin-functionalised imidazoline- and benzimidazoline-NHC ligand have been prepared. The coumarin moiety in the Ir(cod) complexes exhibit a hemilabile behavior through the pyrone ring. Thus, the distorted trigonal bipyramidal geometry observed in the solid state is maintained in solution at low temperature, whereas a square planar isomer was identified at high temperature as a consequence of the decoordination of the coumarin moiety. Both species can be fully characterized by means of NMR spectrometry at the appropriate temperature. In contrast, hemilability was not observed for the bis-CO derivative. The newly synthesized complexes efficiently catalyze the hydrosilylation of alkynes at room temperature with a preference for the β-(Z) vinylsilane isomer. The related rhodium analogues bearing coumarin-NHC ligands but lacking of hemilabile behavior result less efficient. Further studies are underway in our laboratories in order to better understand the actual mode of action of coumarin functionality and its extension to other C-C and C-Heteroatom coupling transformations.

Experimental

General Considerations

All reactions were carried out with rigorous exclusion of air using Schlenk-tube techniques. The reagents were purchased from commercial suppliers and were used as received. The coumarin-functionalized azolium salts were prepared from the corresponding (4-chloromethylene)coumarin derivatives following the procedure recently described.[15] [Ir(μ-OMe)(cod)]$_2$ was synthesized by the procedure described in literature.[28] Organic solvents were dried by standard methods and distilled under argon prior to use or obtained oxygen- and water-free from a Solvent Purification System (Innovative Technologies). Chemical shifts (expressed in parts per million) are referenced to residual solvent peaks (^{1}H, ^{13}C{^{1}H}). Coupling constants, J, are given in Hz. Spectral assignments were achieved by a combination of ^{1}H-^{1}H COSY, ^{13}C{^{1}H}-APT and ^{1}H-^{13}C HSQC/HMBC experiments. High-resolution mass spectra ESI (HRMS-ESI) were recorded using a Bruker MicroTOF-Q equipped with an API-ESI source and a Q-TOF mass analyzer. Infrared spectra were recorded on a Perkin Elmer Spectrum 100 spectrometer, using a Universal ATR Sampling Accessory (neat samples).

Synthesis and characterization data of Iridium-NHC complexes
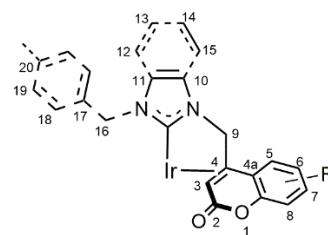
General Method. A yellow solution of [Ir(μ-OMe)(cod)]$_2$ (0.150 mmol) in THF (20 mL) was treated with the corresponding coumarin-functionalized azolium chloride salt (0.300 mmol) and stirred at room temperature for 16 h. After this period, the solution was filtered through celite and concentrated to *ca*. 1 mL. Then, *n*-hexane was added to induce the precipitation of the complexes which were washed with *n*-hexane (3 x 5 mL) and dried in vacuo.

Preparation of IrCl($\kappa C,\eta^2$-I^MeCou^{7,8-Me2})(cod) (4a). Yield: 130 mg (72%). HRMS (ESI, m/z): Calcd for $C_{24}H_{28}IrN_2O_2$ (M-Cl): 569.1775, Found: 569.1785. ^{1}H NMR (400 MHz, CDCl$_3$, 213 K): δ 7.46 (d, J_{H-H} = 8.1, 1H, H$_5$), 7.16 (s, 1H, H$_{10}$), 7.01 (d, J_{H-H} = 8.1, 1H, H$_6$), 6.84 (s, 1H, H$_{11}$), 4.81 and 3.69 (both m, 2H, H$_9$), 4.80, 3.62, 3.61, and 3.13 (all m, 4H, =CH$_{cod}$), 4.05 (s, 3H, NMe), 3.41 (s, 1H, H$_3$), 2.93, 2.41, 2.38, 2.34, 2.08, 1.70, 1.01, and 0.87 (all m, 8H, CH$_{2-cod}$), 2.28 (s, 3H, ArMe$_7$), 2.26 (s, 3H, ArMe$_8$). ^{13}C{^{1}H}-APT NMR (100.4 MHz, CDCl$_3$, 213 K): δ 168.9 (C=O), 155.1 (Ir-C$_{NHC}$), 147.9 (C$_{8a}$), 137.3 (C$_7$), 125.6 (C$_6$), 125.0 (C$_8$), 124.2 (C$_{11}$), 122.6 (C$_{4a}$), 121.7 (C$_5$), 118.8 (C$_{10}$), 105.6, 101.4, 60.4 and 56.2 (=CH$_{cod}$), 54.1 (C$_9$), 52.8 (C$_4$), 39.0 (C$_3$), 38.4, 33.2, 28.6, and 25.7 (CH$_{2cod}$), 37.7 (NMe), 20.9 (ArMe$_7$), 12.6 (ArMe$_8$).

IrCl($\kappa C,\eta^2$-I^MeCou^{6-OMe})(cod) (4b). Yield: 110 mg (60%). Anal. Calcd for $C_{23}H_{26}ClIrN_2O_3$: C, 45.58; H, 4.32; N, 4.62. Found: C, 45.33; H, 4.41; N, 4.47. HRMS (ESI, m/z): Calcd for $C_{23}H_{26}IrN_2O_3$ (M-Cl): 571.1568, Found: 571.1554. ^{1}H NMR (400 MHz, CDCl$_3$, 213 K): δ 7.18 (d, J_{H-H} = 2.6, 1H, H$_7$), 7.16 (d, J_{H-H} = 1.7 Hz, 1H, H$_{10}$), 7.09 (d, J_{H-H} = 8.8, 1H, H$_8$), 6.90 (dd, J_{H-H} = 8.8, 2.6, 1H, H$_5$), 6.85 (d, J_{H-H} = 1.7, 1H, H$_{11}$), 4.85, 3.78, 3.71, and 3.27 (all m, 4H, =CH$_{cod}$), 4.78 and 3.70 (both d, J_{H-H} = 13.2, 2H, H$_9$), 4.07 (s, 3H, NMe), 3.84 (s, 3H, ArOMe), 3.40 (s, 1H, H$_3$), 2.94, 2.46, 2.43, 2.37, 2.12, 1.74, 1.10, and 1.02 (all m, 8H, CH$_{2-cod}$). ^{13}C{^{1}H}-APT NMR (100.4 MHz, CDCl$_3$, 213 K): δ 169.0 (C=O), 155.9 (C$_6$), 154.6 (Ir-C$_{NHC}$), 143.9 (C$_{8a}$), 126.5(C$_{4a}$), 124.3 (C$_{11}$), 118.2 (C$_{10}$), 118.1 (C$_8$), 112.6 (C$_5$), 109.9 (C$_7$), 106.4, 101.7, 61.0, and 56.5 (=CH$_{cod}$), 56.0 (ArOMe), 54.1 (C$_9$), 51.2 (C$_4$), 38.8 (C$_3$), 38.6, 33.3, 28.6 ,and 25.7 (CH$_{2-cod}$), 37.7 (NCH$_3$).

IrCl($\kappa C,\eta^2$-I^VinCou^{7,8-Me2})(cod) (4c). Yield: 90 mg (49%). Anal. Calcd for $C_{25}H_{28}ClIrN_2O_2$: C, 48.73; H, 4.58; N, 4.55. Found: C, 48.57; H, 4.52; N, 4.41. HRMS (ESI) m/z Calcd for $C_{25}H_{28}IrN_2O_2$ (M-Cl): 581.1775, Found: 581.1754. ^{1}H NMR (400 MHz, CDCl$_3$, 213 K): δ 8.42 (dd, J_{H-H} = 15.7 and 8.7, 1H, NCH=CH$_2$), 7.47 (d, J_{H-H} = 8.1, 1H, H$_5$), 7.25 and 7.23 (both s, 2H, H$_{10}$ and H$_{11}$), 7.04 (d, J_{H-H} = 8.1, 1H, H$_6$), 5.18 (d, J_{H-H} = 15.7, 1H, CH=CH$_{2-trans}$), 4.98 (d, J_{H-H} = 8.7, 1H, CH=CH$_{2-cis}$), 4.89, 3.67, 3.65, and 3.19 (all m, 4H, =CH$_{cod}$), 4.87 and 3.70 (both d, J_{H-H} = 13.5, 2H, H$_9$), 3.48 (s, 1H, H$_3$), 2.95, 2.46, 2.39, 2.36, 2.10, 1.73, 1.06, and 0.95 (all m, 8H, CH$_{2-cod}$), 2.30 (s, 3H, ArMe$_7$), 2.28 (s, 3H, ArMe$_8$). ^{13}C{^{1}H}-APT NMR (100.4 MHz, CDCl$_3$, 213 K): δ 168.7 (C=O), 157.0 (Ir-C$_{NHC}$), 147.8 (C$_{8a}$), 137.5 (C$_7$), 133.1 (NCH=CH$_2$), 125.6 (C$_6$), 125.4 (C$_8$), 122.4 (C$_{4a}$), 121.7 (C$_5$), 118.8 and 118.7 (C$_{10}$ and C$_{11}$), 106.2, 101.9, 61.1, and 56.3 (=CH$_{cod}$), 102.8 (NCH=CH$_2$), 54.1 (C$_9$), 52.7 (C$_4$), 39.1 (C$_3$), 38.4, 33.4, 28.5, and 25.7 (CH$_{2-cod}$), 21.0 (ArMe$_7$), 12.7 (ArMe$_8$).

IrCl($\kappa C,\eta^2$-I^BuCou^{7,8-Me2})(cod) (4d). Yield: 100 mg (52%). Anal. Calcd for $C_{27}H_{34}ClIrN_2O_2$: C, 50.18; H, 5.30; N, 4.33. Found: C, 49.85; H, 5.42; N, 4.27. HRMS (ESI) m/z Calcd for $C_{27}H_{34}IrN_2O_2$ (M-Cl): 611.2245, Found: 611.2229. ^{1}H NMR (400 MHz, CDCl$_3$, 213 K): δ 7.45 (d, J_{H-H} = 8.1, 1H, H$_5$), 7.17 (s, 1H, H$_{10}$), 7.01 (d, J_{H-H} = 8.1, 1H, H$_6$), 6.87 (s, 1H, H$_{11}$), 4.82 and 3.68 (both m, 2H, H$_9$), 4.79, 3.65, 3.56, and 3.12 (all m, 4H, =CH$_{cod}$), 4.49 and 4.28 (both m, 2H, NCH$_{2-bu}$), 3.37 (s, 1H, H$_3$), 2.93, 2.42, 2.40, 2.31, 2.07, 1.73, 1.08, and 0.94 (all m, 8H, CH$_{2-cod}$), 2.28 (s, 3H, ArMe$_7$), 2.26 (s, 3H, ArMe$_8$), 1.78 and 1.48 (both m, 2H, NCH$_2$CH$_2$), 1.39 and 1.30 (both m, 2H, CH$_2$CH$_3$), 0.92 (m, 3H, CH$_2$CH$_3$). ^{13}C{^{1}H}-APT NMR (100.4 MHz, CDCl$_3$, 213 K): δ 169.1 (C=O), 155.2 (Ir-C$_{NHC}$), 147.9 (C$_{8a}$), 137.3 (C$_7$), 125.6 (C$_6$), 125.1 (C$_8$), 122.8 (C$_{4a}$), 122.0 (C$_{11}$), 121.7 (C$_5$), 118.4 (C$_{10}$), 105.2, 101.2, 60.4, and 56.0 (=CH$_{cod}$), 54.1 (C$_9$), 52.3 (C$_4$), 49.4 (NCH$_2$), 38.9 (C$_3$), 38.6, 33.2, 28.6, and 26.07 (CH$_{2-cod}$), 34.3 (NCH$_2$CH$_2$), 21.0 (ArMe$_7$), 20.0 (CH$_2$CH$_3$), 14.5 (CH$_2$CH$_3$), 12.7 (ArMe$_8$).

IrCl($\kappa C,\eta^2$-I^BzCou^{7,8-Me2})(cod) (4e). Yield: 130 mg (64%). Anal. Calcd. for $C_{30}H_{32}ClIrN_2O_2$: C, 52.97; H, 4.74; N, 4.12. Found: C, 52.88; H, 4.74; N, 4.03. HRMS (ESI) m/z Calcd for $C_{30}H_{32}IrN_2O_2$ (M-Cl): 645.2089, Found: 645.2106. ^{1}H NMR (400 MHz, CDCl$_3$, 213 K): δ 7.49 (d, J_{H-H} = 8.1, 1H, H$_5$), 7.35 (m, 3H, H$_{m,p-Ph}$), 7.15 (m, 1H, H$_{10}$), 7.11 (d, J_{H-H}= 6.9, 2H, H$_{o-Ph}$), 7.05 (d, J_{H-H} = 8.1, 1H, H$_6$), 6.63 (m, 1H, H$_{11}$), 6.02 and 5.53 (both d, J_{H-H}= 15.8 Hz, 2H, CH$_2$Ph), 4.92 and 3.72 (both d, J_{H-H}= 13.2, 1H, H$_9$), 4.85, 3.85, 3.57, and 3.18 (all m, 1H, =CH$_{cod}$), 3.52 (s, 1H, H$_3$), 2.92, 2.45, 2.42, 2.21, 2.16, 1.63, 1.05, and 0.99 (all m, 8H, CH$_{2-cod}$), 2.30 (s, 3H, ArMe$_7$), 2.28 (s, 3H, ArMe$_8$). ^{13}C{^{1}H}-APT NMR (100.4 MHz, CDCl$_3$, 213 K): δ 169.0 (C=O), 156.4 (Ir-C$_{NHC}$), 147.9 (C$_{8a}$), 137.5 (C$_7$), 136.9 (CH$_2$C$_q$), 129.0, 128.1, and 127.5 (CHPh), 125.7 (C$_6$), 125.2 (C$_8$), 123.0 (C$_{11}$), 122.7 (C$_{4a}$), 121.6 (C$_5$), 118.6 (C$_{10}$), 105.4, 101.5, 60.4, and 56.2 (=CH$_{cod}$), 54.2 (C$_9$), 53.5 (CH$_2$Ph), 52.7 (C$_4$), 39.3 (C$_3$), 38.8, 33.4, 28.5, and 25.7 (CH$_{2-cod}$), 21.0 (ArMe$_7$), 12.7 (ArMe$_8$).

IrCl($\kappa C,\eta^2$-Bzl^TolCou^{7,8-Me2})(cod) (5a). Yield: 120 mg (54%). HRMS (ESI) m/z Calcd for $C_{35}H_{36}IrN_2O_2$ (M-Cl): 709.2402, Found: 709.2411. ^{1}H NMR (400 MHz, CDCl$_3$, 213 K): δ 7.59 (d, J_{H-H} = 8.1, 1H, H$_5$), 7.38 (d, J_{H-H} = 8.1, 1H, H$_{15}$), 7.26 (t, J_{H-H} = 8.1, 1H, H$_{14}$), 7.1 (4H, H$_6$, H$_{13}$, and H$_{19}$), 6.90 (d, J_{H-H} = 8.1, 1H, H$_{12}$), 6.86 (3H, H$_{16}$,H$_{18}$), 5.42 (d, J_{H-H}= 17.1, 1H, H$_{16}$), 5.02 and 3.98 (both d, J_{H-H} = 12.9, 1H, H$_9$), 4.94, 3.94, 3.62, and 3.32 (all m, 4H, =CH$_{cod}$), 3.61 (s, 1H, H$_3$), 2.95, 2.49, 2.46, 2.19, 2.17,1.66, 1.08, and 1.00 (all m, 8H, CH$_{2-cod}$), 2.31 (s, 9H, ArMe$_7$, ArMe$_8$ and Me$_{tol}$). ^{13}C{^{1}H}-APT NMR (100.4 MHz, CDCl$_3$, 213 K): δ 168.7 (C=O), 167.7 (Ir-C$_{NHC}$), 147.9 (C$_{8a}$), 137.7 (C$_7$), 137.4 (C$_{20}$), 134.6 (C$_{11}$), 133.1 (C$_{17}$), 132.1 (C$_{10}$), 129.7 (C$_{19}$), 125.8 (C$_{18}$), 125.7 (C$_6$), 125.3 (C$_8$), 124.2 (C$_{14}$), 123.8 (C$_{13}$), 122.6 (C$_{4a}$), 121.9 (C$_5$), 112.7 (C$_{12}$), 110.8 (C$_{15}$), 106.9, 103.1, 60.4, and 56.4 (=CH$_{cod}$), 53.2 (C$_4$), 51.8 (C$_9$), 51.6 (C$_{16}$), 39.8 (C$_3$), 38.9, 33.3, 28.5, and 25.6 (CH$_{2-cod}$), 21.6 (Me$_{tol}$), 21.1 (ArMe$_7$), 12.8 (ArMe$_8$).

IrCl($\kappa C,\eta^2$-Bzl^TolCou^{6,7-Me2})(cod) (5b). Yield: 110 mg (49%). Anal. Calcd for $C_{35}H_{36}ClIrN_2O_2$: C, 56.48; H, 4.88; N, 3.76. Found: C, 56.21; H, 4.53; N, 3.60. HRMS (ESI) m/z Calcd for $C_{35}H_{36}IrN_2O_2$ (M-Cl): 709.2402, Found: 709.2418. ^{1}H NMR (500 MHz, CDCl$_3$, 213 K): δ 7.59 (s, 1H, H$_5$), 7.39 (d, J_{H-H} = 8.1, 1H, H$_{15}$), 7.28 (t, J_{H-H} = 8.1, 1H, H$_{14}$), 7.09 (3H, H$_{13}$ and H$_{19}$), 6.93 (3H, H$_8$, H$_{12}$ and H$_{16}$), 6.81 (d, J_{H-H} = 8.1, 2H, H$_{18}$), 5.37 (d, J_{H-H}= 17.2, 1H, H$_{16}$), 5.05 and 4.02 (both d, J_{H-H} = 12.8, 2H, H$_9$), 4.97, 3.96, 3.61, and 3.40 (all m, 4H, =CH$_{cod}$), 3.62 (1H, H$_3$), 2.94, 2.52, 2.48, 2.18, 2.17, 1.65, 1.12, and 0.99 (all m, 8H, CH$_{2-cod}$), 2.36 (s, 3H, ArMe$_6$), 2.31 (s, 3H, Me$_{tol}$), 2.27 (s, 3H, ArMe$_7$). ^{13}C{^{1}H}-APT NMR (100.4 MHz, CDCl$_3$, 213 K): δ 168.9 (C=O), 167.6 (Ir-C$_{NHC}$), 148.0 (C$_{8a}$), 137.6 (C$_7$), 137.3 (C$_{20}$), 134.6 (C$_{11}$), 133.2 (C$_{17}$), 133.1 (C$_6$), 132.1 (C$_{10}$), 129.7 (C$_{19}$), 125.7 (C$_5$), 125.6 (C$_{18}$), 124.3 (C$_{14}$), 123.8 (C$_{13}$), 122.4 (C$_{4a}$), 118.1 (C$_8$), 112.7 (C$_{12}$), 110.7 (C$_{15}$), 107.3, 103.3, 60.4, and 56.2 (=CH$_{cod}$), 52.7 (C$_4$), 51.6 (C$_9$), 51.5 (C$_{16}$), 40.3 (C$_3$), 40.0, 33.2, 28.5, and 25.5 (CH$_{2-cod}$), 21.5 (Me$_{tol}$), 20.5 (ArMe$_7$), 20.2 (ArMe$_6$).

IrCl(Bzl^TolCou^{6,7-Me2})(cod) (5b'): the complex could be characterized in a mixture **5b':5b** (molar ratio 9:1) under a fast exchange regime at

343K: ^{1}H NMR (500 MHz, CDCl$_3$, 343 K): δ 7.66 (s, 1H, H$_5$), 7.29 (d, J_{H-H} = 7.6, 1H, H$_{18}$), 7.22 (s, 1H, H$_8$), 7.19 (d, J_{H-H} = 7.6, 1H, H$_{19}$), 7.2-7.1 (4H, H$_{12-15}$), 6.63 and 5.62 (both d, J_{H-H}= 17.2, 2H, H$_9$), 6.15 and 6.06 (both d, J_{H-H} = 15.8, 2H, H$_{16}$), 5.58 (s, 1H, H$_3$), 4.88, 4.66, 3.16, and 3.15 (all m, 4H, =CH$_{cod}$), 2.34, 2.15, 1.90, 1.87, 1.84, 1.67, 1.64, and 1.60 (all m, 8H, CH$_2$-cod), 2.46 (s, 3H, ArMe$_6$), 2.44 (s, 3H, ArMe$_7$), 2.37 (s, 3H, Me$_{tol}$). ^{13}C{^{1}H}-APT NMR (100.4 MHz, C$_2$D$_2$Cl$_4$, 363 K): δ 187.0 (Ir-C$_{NHC}$), 161.4 (C=O), 150.7 (C$_{8a}$), 140.9 (C$_7$), 137.1 (C$_{20}$), 134.6 (C$_{11}$), 133.7 (C$_{10}$), 133.0 (C$_6$), 131.6 (C$_{17}$), 129.1 (C$_{19}$), 125.6 (C$_{18}$), 123.5 (C$_5$), 122.8 and 122.7 (C$_{13-14}$), 117.5 (C$_8$), 116.5 (C$_{4a}$), 111.4 (C$_{12}$), 109.6 (C$_{15}$), 95.2 (C$_3$), 92.7, 91.4, 54.7, and 53.0 (=CH$_{cod}$), 51.8 (C$_{16}$), 48.6 (C$_9$), 34.1, 31.7, 29.3, and 27.7 (CH$_2$-cod), 20.5 (Me$_{tol}$), 19.4 (ArMe$_7$), 18.7 (ArMe$_6$).

IrCl(κC,η^2-BzI^{Bu}Cou$^{6,7\text{-Me2}}$)(cod) (5c). Yield: 110 mg (53%). HRMS (ESI) m/z Calcd for C$_{31}$H$_{36}$IrN$_2$O$_2$ (M-Cl): 661.2402, Found: 661.2373. ^{1}H NMR (400 MHz, CDCl$_3$, 213 K): δ 7.53 (s, 1H, H$_5$), 7.4-7.3 (m, 4H, H$_{12-15}$), 6.92 (s, 1H, H$_8$), 5.06 and 4.48 (both m, 2H, NCH$_2$), 4.97, 3.73, 3.69, and 3.34 (all m, 4H, =CH$_{cod}$), 4.92 and 3.93 (both d, J_{H-H}= 12.8 Hz, 2H, H$_9$), 3.52 (s, 1H, H$_3$), 3.00, 2.50, 2.49, 2.39, 2.11, 1.76, 1.11, and 0.98 (all m, 8H, CH$_2$-cod), 2.34 (s, ArMe$_6$), 2.25 (s, ArMe$_7$), 2.11 and 1.45 (both m, 2H, NCH$_2$CH$_2$), 1.55 and 1.47 (both m, 2H, CH$_2$CH$_3$), 0.99 (m, 3H, CH$_2$CH$_3$). ^{13}C{^{1}H}-APT NMR (100.4 MHz, CDCl$_3$, 213 K): δ 169.2 (C=O), 166.4 (Ir-C$_{NHC}$), 147.9 (C$_{8a}$), 137.5 (C$_7$), 134.6 (C$_{11}$), 133.1 (C$_6$), 132.0 (C$_{10}$), 125.6 (C$_5$), 124.1 and 123.6 (C$_{13}$ and C$_{14}$), 122.4 (C$_{4a}$), 118.0 (C$_8$), 112.0 and 110.9 (C$_{12}$ and C$_{15}$), 107.4, 103.0, 60.4, and 56.0 (=CH$_{cod}$), 52.3 (C$_4$), 51.4 (C$_9$), 47.6 (NCH$_2$), 39.5 (C$_3$), 38.8, 33.2, 28.7, and 25.5 (CH$_{2cod}$), 32.9 (NCH$_2$CH$_2$), 20.6 (ArMe7), 20.4 (CH$_2$CH$_3$), 20.2 (ArMe$_6$), 14.5 (CH$_2$CH$_3$).

IrCl(BzI^{Tol}Cou$^{7,8\text{-Me2}}$)(CO)$_2$ (6). Carbon monoxide was bubbled through an orange solution of **5a** (100 mg, 0.13 mmol) in THF (20 mL) at room temperature for 15 min. Then, the solution was filtered through celite and the filtrate concentrated to ca. 1 mL. Addition of n-hexane induced the precipitation of an orange solid which was washed with n-hexane (3 x 5 mL) and dried in vacuo. Yield: 50 mg (54%). Anal. Calcd for C$_{29}$H$_{24}$ClIrN$_2$O$_4$: C, 50.32; H, 3.50; N, 4.05. Found: C, 50.18; H, 3.46; N, 3.92. IR (cm^{-1}): 2059 ν(CO)$_{sym}$, 1981 ν(CO)$_{asym}$, 1737 ν(C=O)$_{coumarin}$. ^{1}H NMR (400 MHz, CDCl$_3$, 213 K): δ 7.56 (d, J_{H-H} = 8.0, 1H, H$_5$), 7.37-7.16 (m, 9H, H$_6$, H$_{12-15}$, and H$_{18-19}$), 6.49 and 5.81 (both d, J_{H-H} = 18.3, 2H, H$_9$), 5.95 (s, 2H, H$_{16}$), 5.53 (s, 1H, H$_3$), 2.47 (s, 3H, ArMe$_7$), 2.43 (s, 3H, ArMe$_8$), 2.34 (s, 3H, Me$_{tol}$). ^{13}C{^{1}H}-APT NMR (100.4 MHz, CDCl$_3$, 213 K): δ 183.9 (Ir-C$_{NHC}$), 180.8 (Ir-CO$_{trans-NHC}$), 167.3 (Ir-CO$_{cis-NHC}$), 161.3 (C=O), 151.5 (C$_{8a}$), 149.2 (C$_4$), 143.2 (C$_7$), 138.6 (C$_{20}$), 133.9 and 133.7 (C$_{10}$ and C$_{11}$), 131.1 (C$_{17}$), 130.0 and 127.3 (C$_{18-19}$), 126.5 (C$_{13}$ and C$_{14}$), 125.7 (s, C$_8$), 125.2 (C$_6$), 120.2 (C$_5$), 114.7 (C$_{4a}$), 112.9 and 111.3 (C$_{12}$ and C$_{15}$), 110.9 (C$_3$), 53.1 (s, C$_{16}$), 48.5 (s, C$_9$), 21.6 (Me$_{tol}$), 21.3 (ArMe$_7$), 12.2 (ArMe$_8$).

Catalytic hydrosilylation reactions

Hydrosilylation catalytic tests were carried out in NMR tubes under argon atmosphere. In a typical procedure, a NMR tube was charged with the catalyst (2 mol %, 4 x 10^{-3} mmol), CDCl$_3$ (0.5 mL), alkyne (0.20 mmol) and hydrosilane (0.22 mmol). The solution was kept in a thermostatic bath at 298 or 333 K and monitored by ^{1}H NMR

spectroscopy. The reaction products were unambiguously characterized on the basis of the $^3J_{H-H}$ coupling constants of the vinylic protons in the NMR spectra and subsequent comparison to literature data. Values of J ranged from 17 to 19 Hz for β-(E), 13 to 16 Hz for β-(Z), and 1 to 3 Hz for α-vinylsilanes.[26-29] Yields and selectivities were determined by ^{1}H NMR spectroscopy.

Crystal Structure Determination. Single crystals of **4b**·2CHCl$_3$ and **5b**·1.75CHCl$_3$ suitable for the X-ray diffraction studies were grown by slow diffusion of hexane into a chloroform solution of the compound. X-ray diffraction data were collected at 100(2) K on a Bruker APEX SMART CCD diffractometer with graphite-monochromated Mo–Kα radiation (λ = 0.71073 Å) using 0.6° ω rotations. Intensities were integrated and corrected for absorption effects with SAINT–PLUS[30] and SADABS[31] programs, both included in APEX2 package. The structures were solved by the Patterson method with SHELXS-97[32] and refined by full matrix least-squares on F^2 with SHELXL-2014,[33] under WinGX.[34]

Crystal data and structure refinement for 4b·2CHCl$_3$. C$_{23}$H$_{26}$ClIrN$_2$O$_3$·2CHCl$_3$, 844.84 g·mol^{-1}, monoclinic, $P2_1/c$, a = 15.4363(11) Å, b = 16.3179(12) Å, c = 12.9166(9) Å, β = 113.8900(10)°, V = 2974.8(4) Å^3, Z = 4, D_{calc} = 1.886 g·cm^{-3}, μ = 5.148 mm^{-1}, F(000) = 1648, yellow prism, 0.150 x 0.090 x 0.080 mm^3, $\theta_{min}/\theta_{max}$ 2.129/28.258°, index range: −20≤h≤20, −21≤k≤21, −17≤l≤17, reflections collected/independent 33168/7145 [R(int) = 0.0555], T_{max}/T_{min} 0.5633/0.4436, data/restraints/parameters 7145/60/409, GoF(F^2) = 1.031, R_1 = 0.0343 [I > 2 σ(I)], wR_2 = 0.0665 (all data), largest diff. peak/hole 0.789/−0.970 e·Å^{-3}. CCDC deposit number 2083329.

Crystal data and structure refinement for 5b·1.75CHCl$_3$. C$_{35}$H$_{36}$ClIrN$_2$O$_2$·1.75 CHCl$_3$, 953.20 g·mol^{-1}, monoclinic, $P2_1/n$, a = 15.4666(9) Å, b = 14.5473(9) Å, c = 15.8594(9) Å, β = 96.0530(10)°, V = 3548.4(4) Å^3, Z = 4, D_{calc} = 1.784 g·cm^{-3}, μ = 4.271 mm^{-1}, F(000) = 1886, yellow prism, 0.250 x 0.130 x 0.040 mm^3, $\theta_{min}/\theta_{max}$ 1.927/28.550°, index ranges: −20≤h≤20, −19≤k≤18, −21≤l≤21, reflections collected/independent 43969/8481 [R(int) = 0.0629], T_{max}/T_{min} 0.6036/0.4667, data/restraints/parameters 8481/0/409, GoF(F^2) = 1.026, R_1 = 0.0378 [I > 2 σ(I)], wR_2 = 0.0885 (all data), largest diff. peak/hole 1.576/−1.175 e·Å^{-3}. CCDC deposit number 2083330.

Conflicts of interest

There are no conflicts to declare

Acknowledgements

Notes and references

1   (a) J. C. Jeffrey, T. B. Rauchfuss, *Inorg. Chem.*, 1979, **18**, 2658-2666; (b) P. Braunstein, F. Naud, *Angew. Chem. Int. Ed.*, 2001, **40**, 680-699; (c) A. J. M. Miller, *Dalton Trans.*, 2017, **46**, 11987-12000, (d) D. F. Baumgardner, W. E. Parks, J. D. Gilbertson, *Dalton Trans.*, 2020, **49**, 960-965; (e) A C. Carrasco, V. Rodríguez-Fanjul, A. M. Pizarro, *Inorg. Chem.*, 2020, **59**, 16454-16466.

2   (a) O. Kühl, *Chem. Soc. Rev.*, 2007, **36**, 592-607; (b) A. T. Normand, K. J. Cavell, *Eur. J. Inorg. Chem.*, 2008, 2781-2800; (c) V. Miranda-Soto, D. B. Grotjahn, A. L. Cooksy, J. A. Golen, C. E. Moore, A. L. Rheingold, *Angew. Chem. Int. Ed.*, 2011, **50**, 631-635; (d) S. Hameury, P. de Frémont, P. Braunstein, *Chem. Soc. Rev.*, 2017, **46**, 632-733; (e) H. F. Cheng, A. I. d'Aquino, J. Barroso-Flores, C. A. Mirkin, *J. Am. Chem. Soc.,* 2018, **140**, 14590-14594; (f) E. Peris, *Chem. Rev.*, 2018, **118**, 9988-10031; (g) F. Schroeter, I. Císařová, J. Soellner, E. Herdtweckc, T. Strassner, *Dalton* Trans., 2018, **47**, 16638-16650; (h) Q. Zhao, G. Meng, S. P. Nolan, M. Szostak, *Chem. Rev.,* 2020, **120**, 1981-2048.

3   (a) F. E. Hahn, C. Holtgrewe, T. Pape, M. Martin, E. Sola, L. A. Oro, *Organometallics*, 2005, **24**, 2203-2209; (b) R. Corberan, M. Sanau, E. Peris, *Organometallics*, 2007, **26**, 3492-3498; (c) A. Zanardi, E. Peris, J. A. Mata, *New. J. Chem.*, 2008, **32**, 120-126; (d) Y. Tian, T. Maulbetsch, R. Jordan, K. W. Törnroos, D. Kunz, *Organometallics*, 2020, **39**, 1221-1229.

4   (a) G. Choi, H. Tsurugi, K. Mashima, *J. Am. Chem. Soc.*, 2013, **135**, 13149-13161; (b) G. Sipos, A. Ou, B. W. Skelton, L. Falivene, L. Cavallo, R. Dorta, *Chem. Eur. J.,* 2016, **22**, 6939-6946.

5   (a) M. C. Perry, X. Cui, M. T. Powell, D.-R. Hou, J. H. Reibenspies, K. Burgess, *J. Am. Chem. Soc.,* 2003, **125**, 113-123. (b) C.-Y. Wang, C.-F. Fu, Y.-H. Liu, S.-M. Peng, S.-T. Liu, *Inorg. Chem.,* 2007, **46**, 5779-5786; (c) H. M. Peng, R. D. Webster, X. Li, *Organometallics*, 2008, **27**, 4484-4493; (d) M. V. Jiménez, J. Fernández-Tornos, J. J. Pérez-Torrente, F. J. Modrego, S. Winterle, C. Cunchillos, F. J. Lahoz, L. A. Oro, *Organometallics*, 2011, **30**, 5493-5508; (e) Z. G. Specht, S. A. Cortes-Llamas, H. N. Tran, C. J. van Niekerk, K. T. Rancudo, J. A. Golen, C. E. Moore, A. L. Rheingold, T. J. Dwyer, D. B. Grotjahn, *Chem. Eur. J.*, 2011, **17**, 6606-6609; (f) G. Mancano, M. J. Page, M. Bhadbhade, B. A. Messerle, *Inorg. Chem.,* 2014, **53**, 10159-10170; (g) K. Riener, M. J. Bitzer, A. Pöthig, A. Raba, M. Cokoja, W. A. Herrmann, F. E. Kühn, *Inorg. Chem.*, 2014, **53**, 12767-12777; (h) D. Wang, R. T. McBurney, I. Pernik, B. A. Messerle, *Dalton Trans.*, 2019, **48**, 13989-13999; (i) M. Huang, Y. Li, J. Liu, X.-B. Lan, Y. Liu, C. Zhao, Z. Ke, *Green Chem.*, 2019, **21**, 219-224.

6   (a) M. Benítez, E. Mas-Marzá, J. A. Mata, E. Peris, *Chem. Eur. J.*, 2011, **17**, 10453-10461; (b) M. Iglesias, P. J. Sanz Miguel, V. Polo, F. J. Fernández-Alvarez, J. J. Pérez-Torrente, L. A. Oro, *Chem. Eur. J.*, 2013, **19**, 17559-17566; (c) G. González Miera, E. Martínez-Castro, B. Martín-Matute, *Organometallics*, 2018, **37**, 636-644; (d) A. I. Ojeda-Amador, J. Munarriz, P. Alamán-Valtierra, V. Polo, R. Puerta-Oteo, M. V. Jiménez, F. J. Fernández-Alvarez, J. Pérez-Torrente, *ChemCatChem*, 2019, **11**, 5524-5535.

7   (a) H. Seo, H.-J. Park, B. Y. Kim, J. H. Lee, S. U. Son, Y. K. Chung, *Organometallics*, 2003, **22**, 618-620; (b) M. Jonek, A. Makhloufi, P. Rech, W. Frank, C. Ganter, *J. Organomet. Chem.*, 2014, **750**, 140-149.

8   (a) L. D. Field, B. A. Messerle, K. Q. Vuong, P. Turner, *Organometallics*, 2005, **24**, 4241-4250; (b) X. Quan, S. Kerdphon, B. B. C. Peters, J. Rujirawanich, S. Krajangsri, J. Jongcharoenkamol, P. G. Andersson, *Chem. Eur. J.*, 2020, **26**, 13311-13316.

9   (a) A. K. Roy, *Adv. Organomet. Chem.*, **2007**, *55*, 1–59; (b) B. Marciniec, H. Maciejewski, C. Pietraszuk, P. Pawluć; In *Applied Homogeneous Catalysis with Organometallic Compounds*; Cornils, B., Herrmann, W. A., Beller, M., Paciello, R., Eds.; Wiley-VCH: Weinheim, Germany, **2017**; pp 569–620.

10 (a) R. Takeuchi, S. Nitta, D. A. Watanabe, *J. Org. Chem.*, 1995, **60**, 3045–3051; (b) B. M. Trost, Z. T. Ball, *J. Am. Chem. Soc.*, 2005, **127**, 17644–17655; (c) M. V. Jiménez, J. J. Pérez-Torrente, M. Isabel-Bartolomé, V. Gierz, F. J. Lahoz, L. A. Oro, *Organometallics*, 2008, **27**, 224-234; (d) S. Dierick, E. Vercruysse, G. Berthon-Gelloz, I. E. Markó, *Chem. Eur. J.,* 2015, **21**, 17073–17078; (e) J. Guo, Z. Lu, *Angew. Chem., Int. Ed.*, 2016, **55**, 10835–10838; (f) X. Zhao, D. Yang, Y. Zhang, B. Wang, J. Qu, *Org. Lett.*, 2018, **20**, 5357-5361; (g) M.-Y. Hu, J. Lian, W. Sun, T.-Z. Qiao, S.-F. Zhu, *J. Am. Chem. Soc.*, 2019, **141**, 4579-4583; (h) B. Sánchez-Page, J. Munarriz, M. V. Jiménez, J. J. Pérez-Torrente, J. Blasco, G. Subias, V. Passarelli, P. Álvarez, *ACS Catal.* 2020, **10**, 13334-13351; (i) B. Sánchez-Page, M. V. Jiménez, J. J. Pérez-Torrente, V. Passarelli, J. Blasco, G. Subias, M. Granda, P. Álvarez, *ACS Appl. Nano Mater*. 2020, **3**, 1640-1655.

11 M. O. Karataş, A. Di Giuseppe, V. Passarelli, B. Alici, J. J. Perez-Torrente, L. A. Oro, I. Ozdemir, R. Castarlenas, *Organometallics*, 2018, **37**, 191-202.

12 (a) C. Kontogiorgis, A. Detsi, D. Hadjipavlou-Litina, *Expert Opin. Ther. Patents*, 2012, **22**, 437-454; (b) S. Emami, S. Dadashpour, *Eur. J. Med. Chem.*, 2015, **102**, 611-630; (c) S. Balcioglu, M. O. Karataş, B. Ates, B. Alici, I. Ozdemir, *Bioorg. Med. Chem. Lett.*, 2020, **30**, 126805.

13 (a) S. R. Trenor, A. R. Shultz, B. J. Love, T. E. Long, *Chem. Rev.*, 2004, **104**, 3059-3077; (b) D. Cao, Z. Liu, P. Verwilst, S. Koo, P. Jangjili, J. S. Kim, W. Lin, *Chem. Rev.*, 2019, **119**, 10403-10519.

14 R. Puerta-Oteo, J. Munarriz, V. Polo, M. V. Jimenez, J. J. Perez-Torrente, *ACS Catal.*, 2020, **10**, 7367-7380.

15 M. S. Frasinyuk, S. P. Bondarenko, V. P. Khilya, *Chem. Nat. Compd.*, 2006, **42**, 142-147.

16 A. W. Addison, T. N. Rao, J. Reedijk, J. van Rijn, G. C. Verschoor, *J. Chem. Soc., Dalton Trans.,* 1984, 1349–1356.

17 A. von Zelewski, *Stereochemistry of Coordination Compounds*; Wiley: Chichester, 1996.

18 R. Azpíroz, L. Rubio-Pérez, A. Di Giuseppe, V. Passarelli, F. J. Lahoz, R. Castarlenas, J. J. Pérez-Torrente, L. A. Oro, *ACS Catal*. 2014, **4**, 4244–4253.

19 (a) A. R. Chianese, X. Li, M. C. Janzen, J. W. Faller, R. H. Crabtree, *Organometallics*, 2003, **22**, 1663-1667; (b) Y.-H. Chang, C.-F. Fu, Y.-H. Liu, S.-M. Peng, J.-T. Chen, S.-T. Liu, *Dalton Trans.*, 2009, 861-867; (c) S. Gulcemal, A. G. Gokce, B. Cetinkaya, *Dalton Trans.*, 2013, **42**, 7305-7311; (d) P. V. Simpson, K. Radacki, H. Braunschweig, U. Schatzschneider, *J. Organomet. Chem.*, 2015, **782**, 116-123.

20 M. Galiana-Cameo, V. Passarelli, J. J. Pérez-Torrente, A. Di Giuseppe, R. Castarlenas, *Eur. J. Inorg. Chem.* 2021, *in press*.

21 (a) L. Busetto, M. C. Cassani, C. Femoni, C.; M. Mancinelli, A. Mazzanti, A.; R. Mazzoni, G. Solinas, *Organometallics,* 2011, **30**, 5258-5272; (b) M. Iglesias, M. Aliaga-Lavrijsen, P. J. Sanz Miguel, F. J. Fernández-Álvarez, J. J. Pérez-Torrente, L. A. Oro, *Adv. Synth. Catal.,* 2015, **357**, 350-354; (c) J. P. Morales-Cerón, P. Lara, J. López-Serrano, L. L. Santos, V. Salazar, E. Álvarez, A. Suárez, *Organometallics,* 2017, **36**, 2460-2469; (d) A. Tyagi, S. Yadav, P. Daw, C. Ravi, J. K. Bera, *Polyhedron,* 2019, **172**, 167-174; D. Rendón-Nava, J. M. Vásquez-Pérez, C. I. Sandoval-Chávez, A. Alvarez-Hernández, D. Mendoza-Espinosa, *Organometallics,* 2020, **39**, 3961–3971.

22 (a) E. Mas-Marzá, M. Sanaú, E. Peris, *Inorg. Chem.*, 2005, **44**, 9961-9967; (b) M. Iglesias, M. Pérez-Nicolás, P. J. Sanz Miguel, V. Polo, F. J. Fernández-Alvarez, J. J. Pérez-Torrente, L. A. Oro, *Chem. Commun.,* 2012, **48**, 9480-9482.

23 W. Gao, S. Ding, *Synthesis*, 2020, **52**, 3549-3563.

24 X. Xie; X. Zhang, W. Gao, C. Meng, X. Wang, S. Ding, *Commun. Chem*. 2019, **2**, 101.

25 M. Navarro, C. A. Smith, M. Albrecht, *Inorg. Chem*. 2017, **56**, 11688–11701.

26 J. J. Pérez-Torrente, D. H. Nguyen, M. V. Jiménez, F. J. Modrego, R. Puerta-Oteo, D. Gómez-Bautista, M. Iglesias, L. A. Oro, *Organometallics,* 2016, **35**, 2410-2422.

27 M. Iglesias, P. J. Sanz Miguel, V. Polo, F. J. Fernández-Alvarez, J. J. Pérez-Torrente, L. A. Oro, *Chem. Eur. J.,* 2013, **19**, 17559-17566.

28 S. D. Robinson, B. L. Shaw, *J. Chem. Soc*., 1965, 4997-5001.

29 (a) Derivatives from n-BuC≡CH: C. H. Jun, R. H. Crabtree, *J. Organomet. Chem*., 1993, **447**, 177-187; (b) Derivatives from PhC≡CH: H. Katayama, K. Taniguchi, M. Kobayashi, T. Sagawa, T. Minami, F. J. Ozawa, *J. Organomet. Chem.,* 2002, **645**, 192-200; (c) Derivatives from $Et_3SiC≡CH$: T. Sudo, N. Asao,V. Gevorgyan, Y. Yamamoto, *J. Org. Chem.* 1999, **64**, 2494-2499; (d) Derivatives from $4-MeO-C_6H_4C≡CH$: A. Hamze, O. Provot, J.-D. Brion, M. Alami, *J. Organomet. Chem*., 2008, **693**, 2789-2797; (e) Derivatives from $4-CF_3-C_6H_4C≡CH$: A. Hamze, O. Provot, J.-D. Brion, M. Alami, *Synthesis*, 2007, 2025-2036.

30 *SAINT+: Area-Detector Integration Software*, version 6.01; Bruker AXS: Madison, WI, 2001.

31 G. M. Sheldrick, *SADABS program*; University of Göttingen: Göttingen, Germany, 1999.

32 G. M. Sheldrick, *SHELXS 97,* University of Göttingen: Göttingen, Germany, 1997.

33 G. M. Sheldrick, *Acta Crystallogr., Sect. C: Struct. Chem*. 2015, **71**, 3−8.

34 L. J. Farrugia, *J. Appl. Crystallogr*. 2012, **45**, 849−854.

FOR TABLE OF CONTENTS USE ONLY